ↂ

Exact few-body results for strongly correlated quantum gases in two dimensions

Xia-Ji Liu,* Hui Hu,† and Peter D. Drummond‡

ARC Centre of Excellence for Quantum-Atom Optics, Centre for Atom Optics and Ultrafast Spectroscopy,
Swinburne University of Technology, Melbourne 3122, Australia

The study of strongly correlated quantum gases in two dimensions has important ramifications for understanding many intriguing phenomena in solid materials, such as high-T_c superconductivity and the fractional quantum-Hall effect. However, theoretical methods are plagued by the existence of significant quantum fluctuations. Here, we present two- and three-body exact solutions for both fermions and bosons trapped in a two-dimensional harmonic potential with an arbitrary s-wave scattering length. These few-particle solutions link in a natural way to the high-temperature properties of many-particle systems via a quantum virial expansion. As a concrete example, using the energy spectrum of few fermions, we calculate the second and third virial coefficients of a strongly interacting Fermi gas in two dimensions, and consequently investigate its high-temperature thermodynamics. Our thermodynamic results may be useful for ongoing experiments on two-dimensional Fermi gases. These exact results also provide an unbiased benchmark for quantum Monte Carlo simulations of two-dimensional Fermi gases at high temperatures.

I. INTRODUCTION

Two-dimensional (2D) strongly correlated quantum gases present unique features from the point of view of many-body physics.[1] Many sophisticated collective phenomena arise because of reduced dimensionality, such as the long-sought Berezinsky-Kosterlitz-Thouless transition[2–4] and high-T_c superconductivity.[5] In addition, particles in 2D can have non-Abelian quantum statistics, which is strikingly different from bosons and fermions. For this reason, a 2D quantum system is a potential platform for topological quantum computation in a way that is naturally immune to decoherence.[6]

Recent experiments with ultracold atoms offer a unique opportunity to investigate this physics in a controllable way.[1,7] In these experiments, one can modify aspects of the underlying geometry and interactions between the atoms at temperatures down to one billionth of a degree above absolute zero. Experimental schemes to produce a 2D atomic quantum gas include a one-dimensional (1D) optical lattice, formed by the superposition of two running laser waves,[8–12] and strongly focused ellipsoidal optical traps. Using the technique of Feshbach resonances,[13] the interatomic interaction can also be changed from infinitely weak to infinitely strong. This has already led to the observation of the crossover from a Bose-Einstein condensate (BEC) to a Bardeen-Cooper-Schrieffer (BCS) superfluid in three dimensions.[1,7]

Theoretical investigations of 2D strongly correlated atomic quantum gases, in particular, the study of superfluidity in atomic Fermi gases, have already attracted intense attention in the past few years.[1,14–20] However, theoretical methods for nonintegrable 2D Fermi systems are limited due to significant quantum fluctuations. Although a mean-field approach combined with perturbation theory are usually adopted in the understanding of the BCS-BEC crossover in three dimensions,[1,7,21–23] they may simply break down in 2D. Other traditional methods in condensed-matter physics, such as exact diagonalization and quantum Monte Carlo simulation, are often less helpful than one may expect, due to the

restriction to finite number of atoms or due to Fermi sign problems. Furthermore, the harmonic trapping potential in ultracold atom experiments, which is used to prevent the atoms from escaping, complicates theoretical treatments.

In this paper, we present a few-particle perspective on strongly correlated 2D systems by exactly solving for the eigenstates of three identical fermions or bosons in a 2D *isotropic* harmonic trap with arbitrary interaction strength. Three-fermion or three-boson problems in three dimensions (3D) have been thoroughly investigated,[24–27] covering many aspects such as the three-body recombination rate (or stability),[28,29] three-body perspective on BEC,[30] and Efimov physics.[31,32] The three-particle problem in low dimensions, however, is less well studied despite its considerable importance. There are very few studies of universal low-energy properties of three identical bosons confined in 2D.[33–36]

Here, by constructing the exact wave functions, we solve and discuss the full exact energy spectrum of three identical trapped fermions or bosons in 2D. As the Efimov effect occurs only when the dimensionality is greater than two,[24] all the states of fermions and bosons that we study have *universal* properties determined by a single parameter: the s-wave scattering length a_{sc}. For three bosons, we find that an attractive interaction leads to two distinct three-boson bound states in the form of a self-bound boson droplet, as predicted by Hammer and Son[35] using a 2D effective-field theory.

Using few-particle exact solutions, we can also solve the problem of a strongly correlated 2D quantum gas at high temperatures, including both thermodynamics[37] and dynamical properties,[38,39] using a quantum virial expansion method.[40] Here, we calculate the second and third virial (expansion) coefficients of a 2D Fermi gas. We then investigate the high-temperature equation of state, including the chemical potential, energy, and entropy, as a function of temperature at a given interaction strength. Our thermodynamics results give valuable insights for ongoing experiments on 2D Fermi gases.[41,42] Further, these results may also provide a useful benchmark for quantum Monte Carlo simulations for

a 2D Fermi gas at high temperatures, where convergence checks are otherwise difficult to obtain.

The paper is organized as follows. In the next section, we present exact solutions for the energy eigenstates of three-fermion and three-boson systems with arbitrary s-wave interaction in an isotropic 2D harmonic trap and discuss the resulting energy spectrum. In Sec. III, we calculate the second and third virial coefficients of a 2D Fermi gas, at a given temperature and interaction strength. Then, in Sec. IV, we investigate the high-temperature thermodynamics of a strongly correlated 2D Fermi gas. Section V is devoted to conclusions and final remarks. In the Appendix, we outline some numerical details of the exact solutions.

II. EXACT FEW-PARTICLE SOLUTIONS IN A 2D HARMONIC TRAP

We consider a 2D few-particle system of either fermions or bosons in an isotropic 2D harmonic trap $V(\rho) = m\omega^2\rho^2/2$ with $\rho = \sqrt{x^2 + y^2}$, where $\vec{\rho}_j = (x_j, y_j)$ is the jth particle coordinate. For low-energy scattering, the *attractive* interactions between atoms can be formally described by a positive s-wave scattering length a_{sc}. For identical fermions, there is no s-wave partial wave interaction due to the Pauli exclusion principle. We thus consider for fermions two different hyperfine (i.e., pseudospin) states with the interaction occurring only for two fermions with *unlike* spins. In the case of a Feshbach resonance, which allows an adjustable interaction strength, we focus on the case of a broad rather than narrow resonance. This allows us to analyze the problem without considering an explicit molecular channel. More generally, the molecular field causing the resonance should be included, leading to a modified two-particle bound-state eigenfunction.[43]

A peculiar feature of 2D interactions is that any attraction, whatever how small, will support a two-particle bound state with binding energy $E_B = 4\hbar^2/[\exp(2\gamma)ma_{sc}^2]$, where $\gamma \simeq 0.577216$ is the Euler constant.[16] The interactions can then be alternatively characterized by the two-particle binding energy E_B. Contrary to the 3D BEC-BCS crossover situation, where the bound state appears only at a certain interaction strength (i.e., unitarity limit), the scattering length a_{sc} in 2D is always *positive* due to the existence of a 2D bound state.

Following the idea introduced into two-body physics by Bethe and Peierls,[44] it is convenient to replace the s-wave interaction by a set of boundary conditions, which in 2D take the form,[14,36,45,46]

$$\lim_{\rho_{ij} \to 0}\left[\rho_{ij}\frac{d}{d\rho_{ij}} - \frac{1}{\ln(\rho_{ij}/a_{sc})}\right]\psi(\vec{\rho}_1, \ldots, \vec{\rho}_N) = 0, \quad (1)$$

when particles i and j are close to each other. Here, $\psi(\vec{\rho}_1, \ldots, \vec{\rho}_N)$ is the wave function of a system of N particles and $\rho_{ij} = |\vec{\rho}_i - \vec{\rho}_j|$. In addition to these Bethe-Peierls boundary conditions, the wave function $\psi(\vec{\rho}_1, \ldots, \vec{\rho}_N)$ satisfies a noninteracting Schrödinger equation,

$$\sum_{i=1}^{N}\left[-\frac{\hbar^2}{2m}\nabla_{\rho_i}^2 + \frac{1}{2}m\omega^2\rho_i^2\right]\psi = E\psi \quad (2)$$

with no two particles at the same coordinate.

A. Two particles in a 2D harmonic trap

As a preliminary study, let us first revisit the two-particle problem.[47] In a harmonic trap, the motion of the center-of-mass $\mathbf{C} = (\vec{\rho}_1 + \vec{\rho}_2)/2$ can be separated from the relative motion, and the relative Hamiltonian is given by

$$\mathcal{H}_{rel} = -\frac{\hbar^2}{2\mu}\nabla_\rho^2 + \frac{1}{2}\mu\omega^2\rho^2, \quad (3)$$

where $\vec{\rho} = \vec{\rho}_1 - \vec{\rho}_2$ is the relative coordinate and $\mu = m/2$ is the reduced mass. The energy level and the corresponding wave function of two-particle system can be written as $E = E_{cm} + E_{rel}$ and $\Psi_{2p}(\mathbf{C}, \vec{\rho}) = \phi_{2p}^{cm}(\mathbf{C})\psi_{2p}^{rel}(\vec{\rho})$, respectively. Here, the subscript "2p" denotes the two-particle problem.

The wave function of center-of-mass motion, $\phi_{2p}^{cm}(\mathbf{C})$, is simply the well-known wave function of 2D harmonic oscillators with $E_{cm} = (2n_{cm} + |m_{cm}| + 1)\hbar\omega$, where the good quantum number n_{cm} and m_{cm} label, respectively, the number of nodes in the radial wave function and the angular momentum of the center-of-mass motion. The relative wave function should be solved by $\hat{H}_{rel}\psi_{2p}^{rel}(\vec{\rho}) = E_{rel}\psi_{2p}^{rel}(\vec{\rho})$, in conjunction with the Bethe-Peierls boundary condition, $\lim_{\rho \to 0}\{d/d\rho - 1/[\rho\ln(\rho/a_{sc})]\}\psi_{2p}^{rel}(\vec{\rho}) = 0$. The relative Hamiltonian has rotational symmetry and thus has a good quantum number of angular momentum m_{rel}. Due to s-wave coupling, it is easy to see that only the $m_{rel} = 0$ branch of the relative wave functions is affected by the interactions, so we focus on this case.

We start by considering the solutions to the free Hamiltonian without including boundary conditions. The free relative Hamiltonian admits two types of solutions, either in terms of the confluent hypergeometric function of the first kind, $\exp(-\rho^2/2d^2)_1F_1(-\nu, 1, \rho^2/d^2)$, or in terms of the Kummer confluent hypergeometric function of the second kind, $\exp(-\rho^2/2d^2)\Gamma(-\nu)U(-\nu, 1, \rho^2/d^2)$, where $d = \sqrt{\hbar/(\mu\omega)}$ is the length scale of the trap, ν is determined by $E_{rel} = (2\nu + 1)\hbar\omega$, and Γ is the gamma function. The first kind of Kummer function $_1F_1$ is regular in the entire space and gives the standard wave function of a 2D harmonic oscillator. In contrast, the second Kummer function U is singular at the origin.

Now, let us include the Bethe-Peierls boundary condition. It is easy to see that one must choose the second type of Kummer solution as the relative function, i.e.,

$$\psi_{2p}^{rel}(\vec{\rho}) \propto \exp\left(-\frac{\rho^2}{2d^2}\right)\Gamma(-\nu)U\left(-\nu, 1, \frac{\rho^2}{d^2}\right). \quad (4)$$

The parameter ν or the relative energy $E_{rel} = (2\nu + 1)\hbar\omega$ is then uniquely determined by the boundary condition. Considering the property $\partial_x U(-\nu, 1, x) = \nu U(1 - \nu, 2, x)$ and the asymptotic behavior of the confluent hypergeometric function at $x \to 0$,

$$U(1 - \nu, 2, x) = -\frac{1}{\nu\Gamma(-\nu)x} + O(x^0), \quad (5)$$
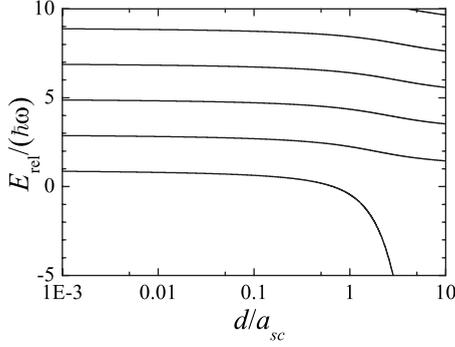
FIG. 1. Relative energy spectrum of a two-particle system with $m_{rel}=0$ as a function of the dimensionless interaction parameter d/a_{sc}. The system goes to the strongly interacting limit when d/a_{sc} increases to an infinitely large value.

$$U(-\nu,1,x)=-\frac{2\gamma+\ln x+\psi(-\nu)}{\Gamma(-\nu)}+O(x^1),$$
$$(6)$$

we immediately obtain the energy equation,

$$\gamma+\frac{1}{2}\psi(-\nu)=\ln\left(\frac{d}{a_{sc}}\right). \qquad (7)$$

Here, $\gamma\simeq0.577216$ is the Euler constant and $\psi(x)$ is the digamma function.

In Fig. 1, we report the relative energy levels of a two-particle system with $m_{rel}=0$ as a function of the dimensionless interaction parameter d/a_{sc}. All the energy levels decrease with increasing interaction strength, as expected for an attractively interacting system. The lowest level corresponds to the ground state of a molecule with size a_{sc} and thus toward the strongly interacting limit (i.e., $a_{sc}\rightarrow0$), it diverges as $-\hbar^2/(ma_{sc}^2)$. All the other excited levels instead converge to the noninteracting limit.

It is interesting to note that with a positive scattering length, the two particles interact repulsively if they do not occupy the ground state of molecules. Thus, by excluding the lowest energy level, Fig. 1 can be alternatively viewed as the energy spectrum of two repulsively interacting particles.[48] Then, the right side with vanishing a_{sc} is the noninteracting limit for the repulsively interacting system and the unitarity limit of infinitely large a_{sc} is the strongly interacting limit.

In the limiting case of either zero or infinite scattering length, one may calculate the asymptotic behavior of energy levels. We find that, for the nth level, the relative energy is given by

$$E_{rel}=\left[2n+1-\frac{2}{2\ln a_{sc}+\gamma+\displaystyle\sum_{k=1}^{n}1/k}\right]\hbar\omega, \qquad (8)$$

where $n=0,1,2,\ldots$ is a non-negative integer and, in the limit of $a_{sc}\rightarrow0$, the lowest molecule state has been excluded in the count of energy levels, so that $n=0$ corresponds to the first excited state.

B. Three fermions in 2D harmonic trap

Let us now turn to the three-particle problem. For three fermions, we consider the configuration with two spin-up fermions (particle 1 and 3) and one spin-down fermion (particle 2), i.e., a ↑↓↑ configuration. It is convenient to use Jacobi coordinates. We define the center-of-mass coordinate $\vec{\rho}_{CM}=(\vec{\rho}_1+\vec{\rho}_2+\vec{\rho}_3)/3$, together with two relative coordinates $\mathbf{r}=\vec{\rho}_1-\vec{\rho}_2$ and $\vec{\rho}=(2/\sqrt{3})[\vec{\rho}_3-(\vec{\rho}_1+\vec{\rho}_2)/2]$. The solution for the center-of-mass motion is again the standard wave function of a 2D harmonic oscillator. For the relative motion, on top of the Bethe-Peierls boundary conditions, the relative Hamiltonian reads[26]

$$\mathcal{H}_{rel}=-\frac{\hbar^2}{2\mu}(\nabla_{\mathbf{r}}^2+\nabla_{\rho}^2)+\frac{1}{2}\mu\omega^2(\mathbf{r}^2+\rho^2). \qquad (9)$$

To solve the three-fermion problem, we extend the approach of Efimov[31] to the trapped case and consider the following relative wave function:[37]

$$\psi_{3f}^{rel}=(1-\mathcal{P}_{13})\chi(\mathbf{r},\vec{\rho}), \qquad (10)$$

where

$$\chi(\mathbf{r},\vec{\rho})=\sum_n a_n^f \psi_{2p}^{rel}(\mathbf{r};\nu_{m,n})R_{nm}(\rho)\frac{e^{im\varphi}}{\sqrt{2\pi}}, \qquad (11)$$

$R_{nm}(\rho)$ is the standard radial wave function of 2D harmonic oscillators with energy $(2n+|m|+1)\hbar\omega$ and the set of parameters $\nu_{m,n}$ is determined by

$$E_{rel}=[(2n+|m|+1)+(2\nu_{m,n}+1)]\hbar\omega, \qquad (12)$$

for a given relative energy E_{rel} and the two good quantum numbers n and m.

The wave function, Eq. (10), is easy to understand. It is simply a summation of products of the wave function of the paired fermions (1 and 3), $\psi_{2p}^{rel}(\mathbf{r};\nu_{m,n})$, and of the wave function of particle 3 relative to the pair, $R_{nm}(\rho)e^{im\varphi}/\sqrt{2\pi}$. The product certainly satisfies the relative Hamiltonian (9) and gives rise to the energy conservation equation for $\nu_{m,n}$, Eq. (12). Owing to the rotational symmetry of the relative Hamiltonian, the angular momentum is well defined and conserved. In the relative wave function, we also include an exchange operator for particle 1 and 3, which ensures the symmetry of the wave function and ensures that the wave function satisfies the Pauli exclusion principle. The set of coefficients a_n^f can be uniquely determined using the Bethe-Peierls boundary conditions. We note that because of the exchange operator, the two boundary conditions reduce to just one, since the other is satisfied automatically.

We now examine the Bethe-Peierls boundary condition which should lead to a secular equation for the energy levels (E_{rel}) and wave functions (a_n^f). Let us consider the first term, $\lim_{r\rightarrow0} r(d/dr)(1-\mathcal{P}_{13})\chi(\mathbf{r},\vec{\rho})$. Recall that $\mathcal{P}_{13}\chi(\mathbf{r},\vec{\rho})=\chi(\mathbf{r}/2-\sqrt{3}\vec{\rho}/2,-\sqrt{3}\mathbf{r}/2-\vec{\rho}/2)$, which is regular at origin. Therefore, we find

$$\lim_{r\rightarrow0}\frac{d\psi_{3f}^{rel}}{dr}=\sum_n a_n^f R_{nm}(\rho)\frac{e^{im\varphi}}{\sqrt{2\pi}}\left[r\frac{d\psi_{2p}^{rel}}{dr}\right]_{r\rightarrow0} \qquad (13)$$

$$= (-2) \sum_n a_n^f R_{nm}(\rho) \frac{e^{im\varphi}}{\sqrt{2\pi}}. \quad (14)$$

On the other hand, in the limit of $r \to 0$,

$$\frac{\psi_{3f}^{rel}}{\ln(r/a_{sc})} = \frac{\chi(\mathbf{r}, \vec{\rho}) - \chi(-\sqrt{3}\vec{\rho}/2, -\vec{\rho}/2)}{\ln(r/a_{sc})}, \quad (15)$$

where effectively $\chi(\mathbf{r}, \vec{\rho})_{r \to 0} = \Sigma_n(-2)[\gamma + \psi(-\nu_{m,n}) + \ln(r/d)]a_n^f R_{nm}(\rho)e^{im\varphi}/\sqrt{2\pi}$. By substituting Eqs. (14) and (15) into the Bethe-Peierls boundary condition, it is easy to show that

$$\sum_n a_n^f \left[B_n R_{nm}(\rho) + R_{nm}\left(\frac{\rho}{2}\right) \psi_{2p}^{rel}\left(\frac{\sqrt{3}\rho}{2}; \nu_{m,n}\right) \right] = 0, \quad (16)$$

where

$$B_n = (-1)^m 2 \left[\gamma + \psi(-\nu_{m,n}) - \ln\left(\frac{d}{a_{sc}}\right) \right]. \quad (17)$$

The above equation can be solved by projecting the left-hand side of the equation onto the expansion basis $R_{n'm}(\rho)$, which is orthogonal and complete. This leads to the secular equation,

$$\sum_{n'} A_{nn'}^f a_n^f = \ln\left(\frac{d}{a_{sc}}\right) a_n^f, \quad (18)$$

where the matrix elements are

$$A_{nn'}^f \equiv [\gamma + \psi(-\nu_{m,n})]\delta_{nn'} + \frac{(-1)^m}{2} C_{nn'} \quad (19)$$

and

$$C_{nn'} \equiv \int_0^\infty \rho d\rho R_{nm}(\rho) R_{n'm}\left(\frac{\rho}{2}\right) \psi_{2p}^{rel}\left(\frac{\sqrt{3}\rho}{2}; \nu_{m,n'}\right). \quad (20)$$

It is clear that $C_{nn'}$ arises from the exchange operator $\mathcal{P}_{13}$. In the absence of $C_{nn'}$, the secular equation is identical in form to Eq. (7), except for an additional degree of freedom which corresponds to the motion of particle 3 relative to the paired fermions (particle 1 and 2). It then describes an *uncorrelated* three-fermion system of a pair and a single particle.

To solve the secular equation, one must imposes a cutoff n_{max} for the number of expansion functions of $R_{nm}(\rho)$. The accuracy of the numerical calculations can be improved by increasing n_{max}. The relative energy level E_{rel} is then implicit in the secular equation via $\nu_{m,n}$. In practice, for a given relative energy level E_{rel}, we diagonalize the matrix $\mathbf{A}_f = \{A_{nn'}^f\}$ to obtain all the possible interaction strengths d/a_{sc} that correspond to this relative energy. We then invert the relations $a_{sc}(E_{rel})$ to calculate the desired energy spectrum (levels) as a function of the interacting strength d/a_{sc}. The main numerical effort is to calculate the matrix elements $C_{nn'}$. We outline the details of this procedure in the Appendix.

We note that, in both the two- and three-body cases, there are noninteracting solutions to the point-contact interaction Hamiltonian. There are many functions that vanish when two particles are at the same point. For the two-particle case, these are the $m > 0$ states. For the three-particle case, the

situation is more complicated. An example as pointed out by Werner and Castin,[25] is the Laughlin state,

$$\psi = e^{-\sum_{i=1}^3 r_i^2/d^2} \prod_{1 \le n < m \le 3} [(x_n + iy_n) - (x_m + iy_m)]^{|\eta|}.$$

These states are not included in our interacting solutions.

C. Three bosons in 2D harmonic trap

For three bosons we can construct a similar relative wave function to Eq. (10). This takes the form

$$\psi_{3b}^{rel} = (1 + \mathcal{P}_{13} + \mathcal{P}_{23})\chi(\mathbf{r}, \vec{\rho}), \quad (21)$$

where

$$\chi(\mathbf{r}, \vec{\rho}) = \sum_n a_n^b \psi_{2p}^{rel}(\mathbf{r}; \nu_{m,n}) R_{nm}(\rho) \frac{e^{im\varphi}}{\sqrt{2\pi}}. \quad (22)$$

Compared with the fermion case, the only difference in the relative wave function is that we need to include two exchange operators with positive sign to enforce the proper symmetry of the bosonic wave function.[25] This modifies the Bethe-Peierls boundary condition and hence the secular equation. Otherwise, we follow the same derivation as in the fermion case. By using $\mathcal{P}_{23}\chi(\mathbf{r}, \vec{\rho}) = \chi(\mathbf{r}/2 + \sqrt{3}\vec{\rho}/2, \sqrt{3}\mathbf{r}/2 - \vec{\rho}/2)$, we find that the secular matrix $\mathbf{A}_b = \{A_{nn'}^b\}$ takes the form

$$A_{nn'}^b \equiv [\gamma + \psi(-\nu_{m,n})]\delta_{nn'} + (-1)^{m+1} C_{nn'}, \quad (23)$$

which has the same structure as $A_{nn'}^f$. The difference is that due to the additional exchange operator and different sign before operators. The prefactor in the $C_{nn'}$ terms is $(-1)^{m+1}$, instead of $(-1)^m/2$ as in Eq. (19).

It is of importance that in two dimensions the three-particle bosonic wave functions we have constructed are universal, in the sense that all the three-boson properties are determined by the single two-body scattering length.[36] This is contrary to the case in three dimensions where even in the zero-range-interaction limit, the Thomas and Efimov effect,[31] results in a set of universal three-boson bound states which are described by an *additional* three-body regularization parameter.[31]

The absence of an Efimov phenomenon, however, does not imply the absence of three-body bound states. In free space, exactly two three-boson bound states appear in two dimensions with an arbitrary two-body s-wave scattering length, in the form of boson droplets.[35] The ground bound state has a binding energy $E_{B3}^{(0)} = 16.522688(1)E_B$ while one excited bound state has $E_{B3}^{(1)} = 1.2704091(1)E_B$. Here, E_B is the two-particle binding energy discussed earlier.

D. Energy spectrum

We now discuss the resulting energy spectrum of three fermions or three bosons. Typically, we set a cutoff $n_{max} = 128$ for the number of radial wave functions $R_{nm}(\rho)$ kept in the calculation. By doubling and halving the value of n_{max}, we have checked that the relative accuracy of energy levels
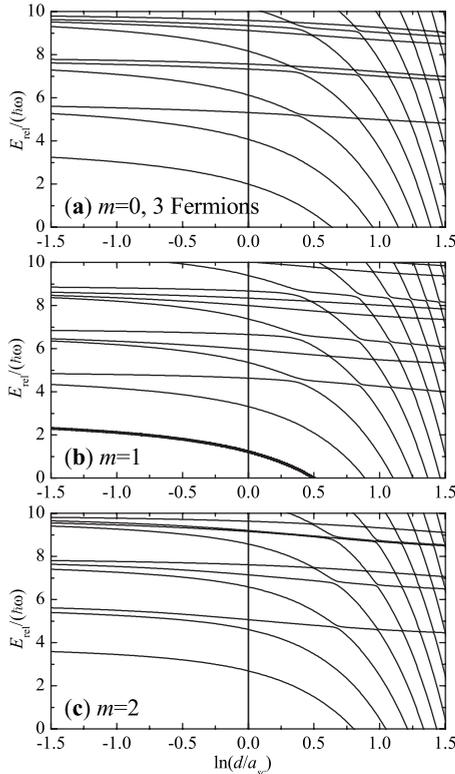
FIG. 2. Relative energy spectrum of three trapped interacting fermions in 2D, as a function of the dimensionless interaction parameter $\ln(d/a_{sc})$. We show the spectrum in different subspaces of relative angular momentum m. The ground-state energy level in the subspace $m=1$ has been highlighted by a thick line.

is less than $<10^{-6}$, except for the $m=0$ subspace for bosons, where the appearance of two three-boson bound states significantly decreases the numerical accuracy.

1. Three-fermion spectrum

Figure 2 gives the relative energy spectrum of a three-fermion system at different relative angular momentum m, as a function of the interaction strength, $\ln(d/a_{sc})$. The ground state is in the subspace $m=1$ due to the Pauli exclusion principle which prohibits all three fermions from interacting when $m=0$, as highlighted by a thick solid line. Compared with the two-body relative energy spectrum, the energy levels are much more complicated. We observe two distinct energy levels with decreasing scattering length and therefore increasingly attractive interaction strengths. Some diverge to $-\infty$ as a_{sc}^{-2} while the others saturate to the limiting values that correspond to the noninteracting energy spectrum. This essential feature exactly resembles what we observed for the two-body relative energy spectrum shown in Fig. 1, where the ground state of two particles diverges to infinitely negative energy, while the other excited states converge to the ideal, noninteracting spectrum. We note that the same feature has also been observed very recently in calculations of a trapped three-fermion system in 3D.[49]

We may therefore identify the diverging energy level as the state that contains a tightly bounded pair or molecule, together with a fermion rotating around the molecule. The energy spacing of this "molecule and atom" state is roughly $2\hbar\omega$, accounting for the rotational degree of freedom of the fermion. Accordingly, the other saturating energy level is a state of three individual fermions, which therefore should interact repulsively. In analogy to the two-particle case, we may regard these "individual atom" states as the energy states of three *repulsively* interacting fermions with the same (positive) s-wave scattering length, although there are necessarily many avoided crossings between the molecule and atom states and the individual atom states. These appear particularly when the scattering length a_{sc} becomes comparable with the characteristic length scale of the harmonic trap, d.

With this classification of energy levels in mind, the spectrum at the limiting cases of $a_{sc} \rightarrow \infty$ and $a_{sc} \rightarrow 0$ are easy to interpret. The former is simply the energy spectrum of three weakly attractively interacting fermions, which, analogous to the two-particle case, decrease linearly as $1/\ln(a_{sc})$ with decreasing a_{sc}. The latter, excluding the molecule and atom states, is the spectrum of three weakly repulsively interacting fermions, increasing linearly as $1/\ln(a_{sc})$ with increasing a_{sc}. It is readily seen that in these two limiting cases the energy levels, together with their degeneracy, are connected smoothly with the spectrum of three ideal, noninteracting fermions.

2. Three-boson spectrum

Figure 3 presents the evolution of the relative energy spectrum of three bosons with increasingly attractive interaction strength. In this case, without the restriction of the Pauli exclusion principle, the ground state is in the subspace of zero relative angular momentum, $m=0$. We highlight this again by using a thick line. The essential features of the spectrum are the same as in the spectrum for three fermions. We observe both the molecule and atom branch and the horizontal individual atom branch, together with some avoided crossings between them. The latter branch may be viewed as the spectrum of three repulsively interacting bosons.

However, there is an important difference, occurring in ground-state subspace with $m=0$. The lowest two states in the molecule and atom branch are three-boson bound states. One is the ground state and the other is the lowest excited state. Their energy is lower than the total energy of two attractively interacting bosons and a third free-moving boson. In particular, the ground-state energy is significantly lower in magnitude than the two-body binding energy E_B. As a result of these three-particle bound states, high numerical accuracy is difficult to obtain. As shown in Fig. 3(a), the energy levels of the two bound states do not converge well even for the largest expansion basis ($n_{\max}=256$) considered in these calculations.

The two bound states describe a self-bound bosonic droplet formed via the attractive, short-ranged two-body potential, resembling the well-known bright soliton of attractive bosons in 1D. Contrary to the Efimov state, these bound states are universal and their properties are determined entirely by the single s-wave scattering length.

We have estimated the binding energy of the two bound states at $\ln(d/a_{sc})=1$ by extrapolating the energy level obtained at a finite expansion basis to $n_{\max}=\infty$. The interaction
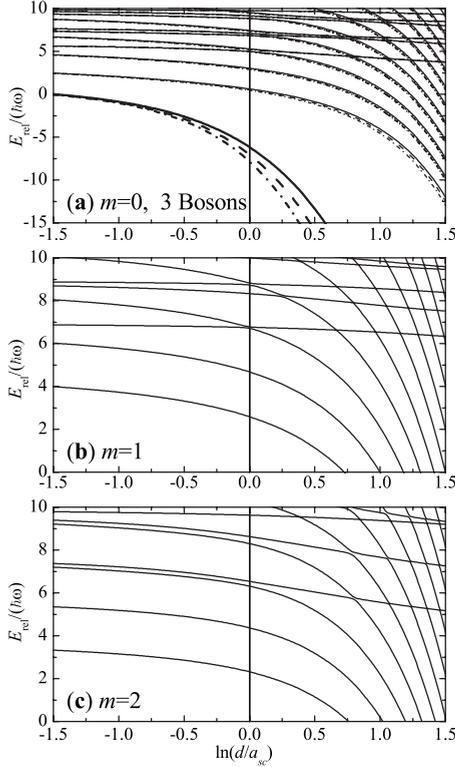
FIG. 3. Relative energy spectrum of three trapped interacting bosons in 2D at difference subspace, as a function of the dimensionless interaction parameter $\ln(d/a_{sc})$. The ground-state energy level in the subspace $m=0$ has been highlighted by a thick line. The numerical accuracy with $m=0$ is greatly suppressed due to the existence of the self-bound dropletlike states. We thus plot the spectrum with $n_{max}=64$ (solid lines), 128 (dashed lines), and 256 (dotted-dashed lines), to show the slow convergence with respect to the number of expansion basis elements n_{max}.

strength is chosen to minimize the influence of the harmonic trap so that the size of the bound state ($\sim a_{sc}$) is much smaller the trapping scale ($\sim d$) while at the same time to maintain the numerical result as accurate as possible. Empirically, we find that the binding energy scales like, $E_{B3}(n_{max}) - E_{B3}(\infty) \propto n_{max}^{-1/4}$. This leads to $E_{B3}^{(0)} \simeq 15.1 E_B$ and $E_{B3}^{(1)} \simeq 1.25 E_B$, which are reasonably in agreement with the accurate binding energies in homogeneous space, $E_{B3}^{(0)} = 16.522688(1) E_B$ and $E_{B3}^{(1)} = 1.2704091(1) E_B$, as predicted by a 2D bosonic effective-field theory.[35] The discrepancy, particularly for the ground-state binding energy, mainly comes from our insufficient numerical accuracy.

III. VIRIAL COEFFICIENTS OF STRONGLY CORRELATED FERMIONS IN 2D

The knowledge of few-particle exact solutions provides a useful input for investigating the high-temperature behavior of a strongly correlated quantum gas, by applying a quantum virial expansion to the thermodynamic properties[37] or dynamical properties.[38,39] Here, we are interested in the high-temperature equation of state of strongly correlated fermions, which are now being accessed experimentally in several laboratories.

The essential idea of the quantum virial expansion is that at high temperatures where the chemical potential μ is strongly negative, the fugacity $z \equiv \exp(\mu/k_B T) \equiv \exp(\beta\mu) \ll 1$ is a well-defined small parameter. We can therefore expand the thermodynamic potential Ω of a quantum system in powers of the fugacity, however strong the interaction strength is. Quite generally, we may write[37]

$$\Omega = -k_B T Q_1 [z + b_2 z^2 + \cdots + b_n z^n + \cdots], \quad (24)$$

where b_n is the nth (virial) expansion coefficient and takes the following form:

$$b_2 = (Q_2 - Q_1^2/2)/Q_1, \quad (25)$$

$$b_3 = (Q_3 - Q_1 Q_2 + Q_1^3/3)/Q_1, \text{ etc.} \quad (26)$$

Here, $Q_n = \text{Tr}_n[\exp(-\mathcal{H}/k_B T)]$ is the partition function of a cluster that contain n particles and the trace Tr_n is taken over all the n-particle states of a proper symmetry. It is clear that Q_n and hence b_n can be calculated once the energy spectrum of up to n-body clusters is known. All the other thermodynamic properties can then be derived from Ω via the standard thermodynamic relations.

In a practical calculation, it is more convenient to focus on how the virial coefficients are affected by interactions. We then may consider the differences $\Delta Q_n = Q_n - Q_n^{(1)}$ and $\Delta b_n = b_n - b_n^{(1)}$, where the superscript "1" denotes an ideal, noninteracting system having the same fugacity. As noted in the previous section, our spectrum of the eigenstates does not include the noninteracting solutions to the boundary-value problem. We deal with this issue by removing these states from both the interacting and noninteracting summations that make up the trace differences ΔQ_n. Since they have the same energy with or without interactions, this does not affect our results. Accordingly, we may rewrite the thermodynamic potential in the form

$$\Omega = \Omega^{(1)} - k_B T Q_1 [\Delta b_2 z^2 + \cdots + \Delta b_n z^n + \cdots], \quad (27)$$

where $\Omega^{(1)}$ is the noninteracting thermodynamic potential with the same fugacity and

$$\Delta b_2 = \Delta Q_2/Q_1, \quad (28)$$

$$\Delta b_3 = \Delta Q_3/Q_1 - \Delta Q_2, \text{ etc.} \quad (29)$$

We now describe how to calculate the noninteracting thermodynamic potential $\Omega^{(1)}$ and the virial coefficients Δb_n.

A. Noninteracting thermodynamic potential $\Omega^{(1)}$

Let us consider a two-component noninteracting Fermi gas in the thermodynamic limit. In the limit of a large number of fermions, the noninteracting thermodynamic potential $\Omega^{(1)}$ is given *semiclassically* by

$$\Omega^{(1)} = -\frac{2}{\beta} \int \frac{d\vec{\rho}\,d\mathbf{k}}{(2\pi)^2} \ln[1 + e^{-\beta[(\hbar^2 k^2/2m)+(m/2)\omega^2\rho^2-\mu]}] \quad (30)$$

$$= -2\frac{(k_B T)^3}{(\hbar\omega)^2}\int_0^\infty t\ln(1+ze^{-t})dt. \tag{31}$$

Subsequently, the number of atoms, $N^{(1)}=-\partial\Omega^{(1)}/\partial\mu$, and the entropy, $S^{(1)}=-\partial\Omega^{(1)}/\partial T$, may be calculated, as well as the total energy, $E^{(1)}=\Omega^{(1)}+TS^{(1)}+\mu N^{(1)}$. We find that

$$N^{(1)} = -2\left(\frac{k_B T}{\hbar\omega}\right)^2\int_0^\infty t\frac{ze^{-t}}{1+ze^{-t}}dt \tag{32}$$

and

$$E^{(1)} = 2\frac{(k_B T)^3}{(\hbar\omega)^2}\int_0^\infty t^2\frac{ze^{-t}}{1+ze^{-t}}dt = -2\Omega^{(1)}. \tag{33}$$

B. Second virial coefficient Δb_2

We now calculate the second virial coefficient. We are interested in the limit of a large number of fermions ($N \gg 1$), a situation that will mostly likely happen in experiment. As the Fermi energy E_F or the Fermi temperature $T_F = E_F/k_B$ is given by $E_F = N^{1/2}\hbar\omega$ and the temperature $T \sim T_F$, we shall define a reduced trapping frequency $\tilde\omega = \hbar\omega/k_B T \ll 1$. The thermodynamic limit is reached in the limit of $\tilde\omega \to 0$. In this limit, the single-particle partition function, determined by the single-particle spectrum for a 2D harmonic oscillator $E_{nm}=(2n+|m|+1)\hbar\omega$ is given by $Q_1=2/(e^{+\tilde\omega/2}-e^{-\tilde\omega/2})\simeq 2(k_B T)^2/(\hbar\omega)^2$, which can also be determined from the first-order expansion of the noninteracting thermodynamic potential $\Omega^{(1)}$. The prefactor of two accounts for the two possible spin states of a single fermion.

The second virial coefficient Δb_2 is given by ΔQ_2. It is readily seen that the summation over the center-of-mass energy in Q_2 gives exactly $Q_1/2$. Using the relative two-body energy $E_{rel}=(2\nu_n+1)\hbar\omega$, where ν_n is nth solution of Eq. (7), we find that

$$\Delta b_2 = \frac{1}{2}\sum_{\nu_n}\left[e^{-(2\nu_n+1)\tilde\omega}-e^{-(2\nu_n^{(1)}+1)\tilde\omega}\right], \tag{34}$$

where the noninteracting $\nu_n^{(1)}=n$ ($n=0,1,2,\ldots$) is a nonnegative integer.

C. Third virial coefficient Δb_3

The third virial coefficient, given by $\Delta b_3 = \Delta Q_3/Q_1 - \Delta Q_2$, is more difficult to calculate. Both the term $\Delta Q_3/Q_1$ and ΔQ_2 diverge as $\tilde\omega \to 0$ with the leading divergences canceling each other. We thus have to separate out carefully the leading terms and treat them analytically. It is easy to see that the spin configurations of $\uparrow\downarrow\uparrow$ and $\downarrow\uparrow\downarrow$ contribute equally to Q_3. As Q_1 in the denominators cancels exactly with the summation over the center-of-mass energy, we have $\Delta Q_3/Q_1 = [\Sigma\exp(-E_{rel}/k_B T) - \Sigma\exp(-E_{rel}^{(1)}/k_B T)]$. To calculate this, it turns out to be important to analyze the behavior of E_{rel} at large energies.

To this aim, we define a relative energy $\bar E_{rel}$, which is the solution of Eq. (19) without the exchange term C_{nm}. The utility of $\bar E_{rel}$ is that it can be constructed directly from the
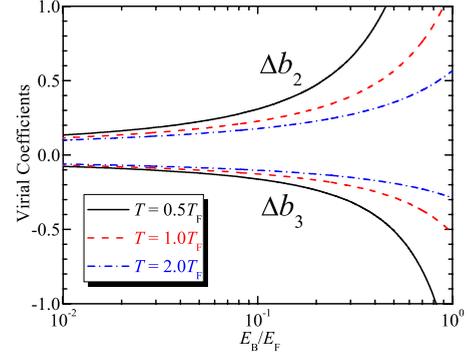
FIG. 4. (Color online) Second and third virial coefficients as a function of the interaction strength E_B/E_F at different temperatures, $T/T_F=0.5$ (solid lines), 1.0 (dashed lines), and 2.0 (dotted-dashed lines).

two-body relative energy. In the subspace with a total relative momentum m, it takes the form

$$\bar E_{rel} = (2n+|m|+1)\hbar\omega + (2\nu+1)\hbar\omega, \tag{35}$$

where ν is the solution of the two-particle spectrum, Eq. (7). At large energies where the exchange effect becomes less important, the full spectrum E_{rel} approaches $\bar E_{rel}$ asymptotically. There is an exception, however, at zero total relative momentum $m=0$. The solution of $\bar E_{rel}$ at $n=0$ and $m=0$ is spurious, due to the exchange operator which leads to a vanishing relative wave function. It therefore cannot match any solution of E_{rel}. In the $m=0$ subspace, we must require $n \geq 1$ in Eq. (35).

Interestingly, if we retain the spurious solution in the $m=0$ subspace, the difference $[\Sigma\exp(-\bar E_{rel}/k_B T)-\Sigma\exp(-E_{rel}^{(1)}/k_B T)]$ gives ΔQ_2 exactly, since the first part in Eq. (35) is identical to the spectrum of center-of-mass motion. The spurious solution gives the contribution,

$$\sum_{\nu_n}\left[e^{-(2\nu_n+2)\tilde\omega}-e^{-(2\nu_n^{(1)}+2)\tilde\omega}\right] \equiv 2e^{-\tilde\omega}\Delta b_2, \tag{36}$$

which should be subtracted. We thus finally arrive at the following expression for the third virial coefficient:

$$\Delta b_3 = \sum\left[e^{-E_{rel}/k_B T}-e^{-\bar E_{rel}/k_B T}\right] - 2e^{-\tilde\omega}\Delta b_2. \tag{37}$$

The summation should be taken over all the possible relative energy levels E_{rel} and their asymptotic counterparts $\bar E_{rel}$. It is well behaved at arbitrary interaction strengths.

D. Numerical results of virial coefficients

We have numerically calculated the second and third virial coefficients as functions of interaction strength and temperature with a small reduced trapping frequency $\tilde\omega \ll 1$. To ensure the accuracy of the calculations for Δb_3, we typically use a hundred thousand relative energies E_{rel}. The dependence of the virial coefficients on $\tilde\omega$ may be removed by a careful scaling analysis.

Figure 4 shows the evolution of the virial coefficients with increasing interaction strength, as characterized by the
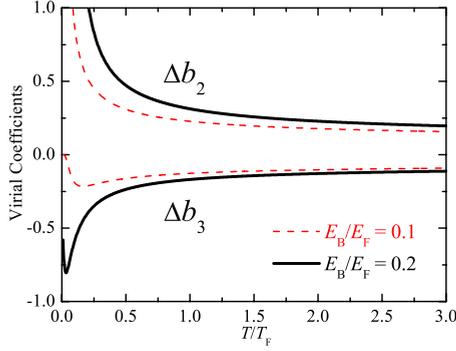
FIG. 5. (Color online) Temperature dependence of the second and third virial coefficients at two interaction strengths, $E_B = 0.2E_F$ (solid lines) and $E_B = 0.1E_F$ (dashed lines).

dimensionless two-body binding energy E_B/E_F. The coefficients diverge exponentially in the strongly attractively interacting limit, due to the formation of tightly bound molecules. The lower the temperature, the faster the divergence.

Figure 5 presents the temperature dependence of the virial coefficients at two interaction strengths, $E_B = 0.2E_F$ and $E_B = 0.1E_F$. The coefficients vary strongly with the temperature in the degenerate regime ($T < T_F$). However, approaching the high-temperature Boltzmann limit ($T \gg T_F$), the coefficients tend to saturate to a semiclassical value.

IV. HIGH-T THERMODYNAMICS OF STRONGLY CORRELATED FERMIONS IN 2D

We are now in position to study the equation of state in the high-temperature regime. Using the thermodynamic relations, it is easy to obtain

$$N = N^{(1)} + 2\left(\frac{k_B T}{\hbar\omega}\right)^2 [2\Delta b_2 z^2 + 3\Delta b_3 z^3 + \cdots] \quad (38)$$

and

$$E = -2\Omega + 2\frac{(k_B T)^3}{(\hbar\omega)^2}\frac{T}{T_F}[\Delta b_2' z^2 + \Delta b_3' z^3 + \cdots], \quad (39)$$

where we have defined $\Delta b_n' \equiv d(\Delta b_n)/d(T/T_F)$ and the Fermi temperature $T_F = \sqrt{N}\hbar\omega/k_B$. The entropy is then calculated by using $S = (E - \Omega - \mu N)/T$, where $\mu = k_B T \ln z$. Equations (27), (38), and (39), together with the noninteracting number, Eq. (32), form a closed set of expressions for thermodynamics.

We perform the calculation at a given fugacity within the trap units $\hbar = m = \omega = k_B = 1$. In the case of thermodynamic limit, the temperature is fixed to an arbitrary constant (i.e., $T = 100$). The virial coefficients and their derivative with respect to the reduced temperature are known as the input. We then calculate N by using the number, Eq. (38), with an initial guess of the reduced temperature T/T_F and obtain in turn the Fermi temperature $T_F = \sqrt{N}$. The reduced temperature T/T_F is updated. We iterate this procedure until the final number of fermions and the reduced temperature converges within a given relative error. We then calculate the total energy using Eq. (39) and consequently the entropy $S = (E - \Omega)/T - Nk_B \ln z$. We finally plot the chemical potential, en-
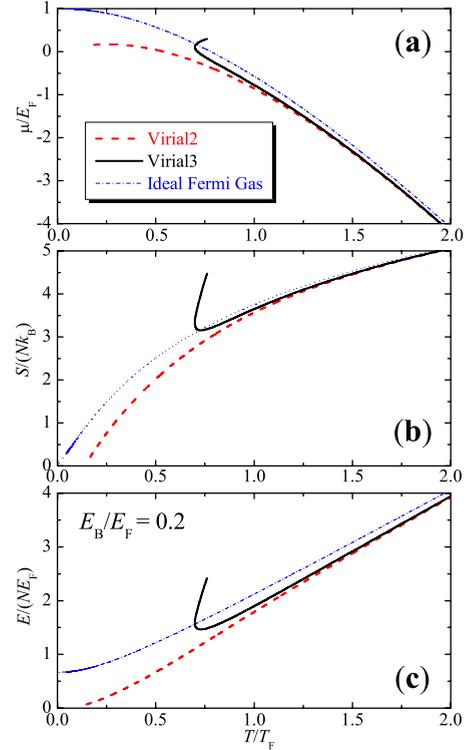
FIG. 6. (Color online) Temperature dependence of the chemical potential, entropy, and energy of a strongly correlated Fermi gas in a 2D harmonic trap. The predictions of virial expansion up to the third and second order are shown, respectively, by the solid lines and dashed lines. For comparison, we also show the ideal, noninteracting results using dotted-dashed lines.

tropy, or energy per particle, μ/E_F, $S/(Nk_B)$, and $E/(NE_F)$, as a function of the reduced temperature T/T_F.

Figure 6 gives the high-temperature equations of state of a strongly correlated 2D Fermi gas at a typical interaction strength $E_B = 0.2E_F$. Compared with the ideal, noninteracting results, the equations of state of a 2D trapped Fermi gas are strongly affected by interactions, even in the high-temperature regime. The applicability of the quantum virial expansion method may be examined by comparing the prediction of expansions of different orders. We estimate conservatively that the third-order virial expansion is reliable down to the Fermi degeneracy temperature, $T \sim T_F$.

V. CONCLUSIONS AND REMARKS

In conclusion, we have presented the exact three-particle energy eigenstates in a two-dimensional harmonic trap, for identical interacting fermions and bosons. The energy spectra have been discussed in detail. We have identified two types of energy levels, one containing a molecule and the other consisting of individual atoms. The latter branch may be interpreted as the energy spectrum of a repulsively interacting system. For three strongly interacting bosons, we have found two universal three-body bound states, corresponding to a self-bound boson droplet. The calculated binding energy of the droplet is in reasonable agreement with a previous theoretical prediction.[35]

Based on these exact solutions, we are able to predict the high-temperature thermodynamics of a strongly correlated quantum gas, by applying a quantum virial expansion method. We have calculated the second and third virial coefficients of a strongly correlated two-dimensional Fermi gas in a harmonic trap and have calculated in turn the temperature dependence of the chemical potential, entropy, and energy. Motivated by the striking experimental confirmation of quantum virial expansion prediction for strongly interacting fermions in three dimensions,[50] we anticipate that our prediction in two dimensions will be tested in future experiments of two-dimensional Fermi gases. Our thermodynamic results may also provide a useful benchmark for future quantum Monte Carlo simulations at high temperatures for two-dimensional systems of ultracold atoms.

APPENDIX: CALCULATION OF $C_{nn'}$

In this appendix, we outline the details of how to construct the matrix element $C_{nn'}$ in Eq. (19), which is given by

$$C_{nn'} \equiv \int_0^\infty \rho \, d\rho R_{nm}(\rho) R_{n'm}\left(\frac{\rho}{2}\right) \psi_{2p}^{rel}\left(\frac{\sqrt{3}}{2}\rho; \nu_{m,n'}\right), \quad \text{(A1)}$$

where

$$R_{nm}(\rho) = \sqrt{\frac{2n!}{(n+|m|)}} \rho^{|m|} e^{-\rho^2/2} L_n^{|m|}(\rho^2) \quad \text{(A2)}$$

is the radial wave function of an isotropic 2D harmonic oscillator and the two-body relative wave function,

$$\psi_{2p}^{rel} = \Gamma(-\nu_{m,n'}) U\left(-\nu_{m,n'}, 1, \frac{3}{4}\rho^2\right) \exp\left(-\frac{3}{8}\rho^2\right). \quad \text{(A3)}$$

Here, for convenience we have set $d=1$ as the unit of length. $L_n^{|m|}$ is the generalized Laguerre polynomial and U is the second Kummer confluent hypergeometric function. A direct integration for $C_{nn'}$ is difficult since the second Kummer function becomes singular close to the origin. Moreover, the integration for different values of $\nu_{m,n'}$ makes the numerical calculation very time consuming.

Thus, it is better to use a different strategy by writing

$$\psi_{2b}^{rel} = \sum_{k=0}^\infty \frac{1}{k - \nu_{m,n'}} \frac{1}{\sqrt{2}} R_{k0}\left(\frac{\sqrt{3}}{2}\rho\right). \quad \text{(A4)}$$

Here, we have used the mathematical identity,

$$\Gamma(-\nu) U(-\nu, 1, x^2) = \sum_{k=0}^\infty \frac{L_k(x^2)}{k - \nu}. \quad \text{(A5)}$$

Therefore, we arrive at

$$C_{nn'} = \sum_{k=0}^\infty \frac{1}{k - \nu_{m,n'}} \frac{1}{\sqrt{2}} C_{nn'k}^m, \quad \text{(A6)}$$

where

$$C_{nn'k}^m \equiv \int_0^\infty \rho \, d\rho R_{nm}(\rho) R_{n'm}\left(\frac{\rho}{2}\right) R_{k0}\left(\frac{\sqrt{3}}{2}\rho\right) \quad \text{(A7)}$$

can be calculated with high accuracy by using an appropriate integration algorithm. We note that, with a cutoff n_{max} for the number of expansion functions (i.e., $n, n' < n_{max}$), $C_{nn'k}^m$ vanishes identically for a sufficient large $k > k_{max} \sim 4n_{max}$. Thus, the summation over k in Eq. (A6) terminates naturally and one does not need to worry about the convergence problem.

In the practical calculation, we tabulate and store the coefficients $C_{nn'k}^m$ in a file, for some given total relative angular momentum m. Thus, the calculation of $C_{nn'}$ for different values of $\nu_{m,n'}$ reduces to a simple summation, which is very efficient and fast. We confirmed numerically that the matrix $C_{nn'}$ is symmetric, i.e., $C_{nn'} = C_{n'n}$. A standard diagonalization algorithm can therefore be adopted for the matrix $\mathbf{A}_f$ or $\mathbf{A}_b$.

*xiajiliu@swin.edu.au

†hhu@swin.edu.au

‡pdrummond@swin.edu.au

[1] I. Bloch, J. Dalibard, and W. Zwerger, Rev. Mod. Phys. **80**, 885 (2008).

[2] V. L. Berezinskii, Sov. Phys. JETP **34**, 610 (1972).

[3] J. M. Kosterlitz and D. J. Thouless, J. Phys. C **6**, 1181 (1973).

[4] Z. Hadzibabic, P. Krüger, M. Cheneau, B. Battelier, and J. Dalibard, Nature (London) **441**, 1118 (2006).

[5] P. A. Lee, N. Nagaosa, and X.-G. Wen, Rev. Mod. Phys. **78**, 17 (2006).

[6] C. Nayak, S. H. Simon, A. Stern, M. Freedman, and S. D. Sarma, Rev. Mod. Phys. **80**, 1083 (2008).

[7] S. Giorgini, L. P. Pitaevskii, and S. Stringari, Rev. Mod. Phys. **80**, 1215 (2008).

[8] C. Orzel, A. K. Tuchmann, K. Fenselau, M. Yasuda, and M. A. Kasevich, Science **291**, 2386 (2001).

[9] S. Burger, F. S. Cataliotti, C. Fort, P. Maddaloni, F. Minardi, and M. Inguscio, Europhys. Lett. **57**, 1 (2002).

[10] M. Köhl, H. Moritz, T. Stöferle, C. Schori, and T. Esslinger, J. Low Temp. Phys. **138**, 635 (2005).

[11] O. Morsch and M. Oberthaler, Rev. Mod. Phys. **78**, 179 (2006).

[12] I. B. Spielman, W. D. Phillips, and J. V. Porto, Phys. Rev. Lett. **98**, 080404 (2007).

[13] C. Chin, R. Grimm, P. Julienne, and E. Tiesinga, Rev. Mod. Phys. **82**, 1225 (2010).

[14] M. Randeria, J. M. Duan, and L. Y. Shieh, Phys. Rev. Lett. **62**, 981 (1989); Phys. Rev. B **41**, 327 (1990).

[15] S. S. Botelho and C. A. R. Sá de Melo, Phys. Rev. Lett. **96**, 040404 (2006).

[16] D. S. Petrov, M. A. Baranov, and G. V. Shlyapnikov, Phys. Rev. A **67**, 031601(R) (2003).

[17] J.-P. Martikainen and P. Törmä, Phys. Rev. Lett. **95**, 170407 (2005).

[18] G. M. Bruun and E. Taylor, Phys. Rev. Lett. **101**, 245301 (2008).

[19] W. Zhang, G.-D. Lin, and L.-M. Duan, Phys. Rev. A **78**, 043617 (2008).

[20] J. Tempere, S. N. Klimin, and J. T. Devreese, Phys. Rev. A **79**, 053637 (2009).

[21] H. Hu, X.-J. Liu, and P. D. Drummond, Europhys. Lett. **74**, 574 (2006).

[22] H. Hu, X.-J. Liu, and P. D. Drummond, New J. Phys. **12**, 063038 (2010).

[23] H. Hu, P. D. Drummond, and X.-J. Liu, Nat. Phys. **3**, 469 (2007).

[24] E. Braaten and H.-W. Hammer, Phys. Rep. **428**, 259 (2006).

[25] F. Werner and Y. Castin, Phys. Rev. Lett. **97**, 150401 (2006).

[26] F. Werner and Y. Castin, Phys. Rev. A **74**, 053604 (2006).

[27] J. P. Kestner and L.-M. Duan, Phys. Rev. A **76**, 033611 (2007).

[28] D. S. Petrov, Phys. Rev. A **67**, 010703(R) (2003).

[29] D. S. Petrov, C. Salomon, and G. V. Shlyapnikov, Phys. Rev. Lett. **93**, 090404 (2004).

[30] D. Blume and C. H. Greene, Phys. Rev. A **66**, 013601 (2002).

[31] V. N. Efimov, Sov. J. Nucl. Phys. **12**, 589 (1971).

[32] For a brief review, see, for example, F. Ferlaino and R. Grimm, Phys. **3**, 9 (2010).

[33] L. W. Bruch and J. A. Tjon, Phys. Rev. A **19**, 425 (1979).

[34] E. Nielsen, D. V. Fedorov, and A. S. Jensen, Phys. Rev. A **56**, 3287 (1997).

[35] H.-W. Hammer and D. T. Son, Phys. Rev. Lett. **93**, 250408 (2004).

[36] O. I. Kartavtsev and A. V. Malykh, Phys. Rev. A **74**, 042506 (2006).

[37] X.-J. Liu, H. Hu, and P. D. Drummond, Phys. Rev. Lett. **102**, 160401 (2009); arXiv:1007.1041, Phys. Rev. A (to be published).

[38] H. Hu, X.-J. Liu, and P. D. Drummond, Phys. Rev. A **81**, 033630 (2010).

[39] H. Hu, X.-J. Liu, and P. D. Drummond, Phys. Rev. Lett. **104**, 240407 (2010).

[40] T.-L. Ho and E. J. Mueller, Phys. Rev. Lett. **92**, 160404 (2004).

[41] P. Dyke, Ph.D. thesis, Swinburne University of Technology, 2010.

[42] K. Martiyanov, V. Makhalov, and A. Turlapov, Phys. Rev. Lett. **105**, 030404 (2010).

[43] K. V. Kheruntsyan and P. D. Drummond, Phys. Rev. A **61**, 063816 (2000).

[44] H. Bethe and R. Peierls, Proc. R. Soc. London, Ser. A **148**, 146 (1935).

[45] S. K. Adhikari, Am. J. Phys. **54**, 362 (1986).

[46] D. S. Petrov and G. V. Shlyapnikov, Phys. Rev. A **64**, 012706 (2001).

[47] T. Busch, B. G. Englert, K. Rzazewski, and M. Wilkens, Found. Phys. **28**, 549 (1998).

[48] R. A. Duine and A. H. MacDonald, Phys. Rev. Lett. **95**, 230403 (2005).

[49] K. M. Daily and D. Blume, Phys. Rev. A **81**, 053615 (2010).

[50] S. Nascimbène, N. Navon, K. J. Jiang, F. Chevy, and C. Salomon, Nature **463**, 1057 (2010).